Supporting Information

Tang et al. 10.1073/pnas.1105547108

SI Text

Buffer and DNA Size Dependence of the Compression. To verify that the electric field induced DNA compression is not caused by the specific interactions between DNA and the boric acid in the TBE buffer (1), we examine the conformation of T4 DNA under uniform DC (direct current) electric field in 1 × TE buffer with 15 mM NaCl. The ionic strength of this buffer is 26 mM, roughly equivalent to that of the 0.5 × TBE buffer (27 mM). Fig. S1 *A* and *B* show the ensemble average radius of gyration (normalized by the equilibrium average) and the corresponding anisotropic ratio of T4 DNA in both buffers as functions of the electric field strength, respectively. Compression of T4 DNA by electric field is also observed in the TE buffer, indicating it is not due to the presence of boric acid in the TBE solution. Under the same electric field strength, T4 DNA in the TE buffer is slightly less compressed. We believe this different extent of compression results from the lower charge density of DNA molecules in the absence of boric acid (1, 2).

We compare the compression of T4 DNA (165.6 kbp) and λ-DNA (48.5 kbp) under uniform DC electric field in 0.5 × TBE. Fig. S1 *C* and *D* show the ensemble average radius of gyration (normalized by the equilibrium average) and the corresponding anisotropic ratio of both types of DNA as functions of the electric field strength, respectively. It is clearly seen that the T4 DNA is significantly more compressed under the same field strength, suggesting that the electric field induced compression is stronger for DNA with a larger molecular weight. The same dependence on DNA size has been observed for the electric field induced intermolecular DNA aggregation in a more concentrated ($\sim c^*$) DNA solution (3).

Properties of DNA Ensembles Compressed Under AC Electric Field. We have studied the expansion of seven T4 DNA ensembles compressed using 10 Hz AC (alternating current) square-wave electric fields with different combinations of root-mean-square electric field strength E_{rms} and duration T_E. Table S1 summarizes the initial average radius of gyration $\langle R_{g,0}\rangle$ and the proportion of DNA molecules exhibiting type II expansion for each DNA ensemble. We use a simple mathematic standard to distinguish the two types of expansion: the expansion of a DNA molecule is classified as type I if its radius of gyration reaches the equilibrium average within 8 s. The proportion of DNA following type II expansion pathway increases when the ensemble is subject to either a longer duration or stronger strength of electric field. The observed slowdown of the average expansion process with increasing T_E or E_{rms} essentially results from two facts: (*i*) more DNA molecules become entangled and thus transition to the much slower type II expansion, and (*ii*) the number of entanglements within a DNA molecule increases which further slows down the expansion.

Data Analysis for Type II Expansion of Compressed T4 DNA. ***Determining onset of stage 2 and stage 3.*** We determined the onset of stage 2 and stage 3 based on the distinct degrees of DNA fluctuation in the three stages of type II expansion. For each individual R_g trace, we calculated the standard deviation σ of the local 2 s of R_g data at every time point with a sliding window 1 s ahead to 1 s after. We then used two threshold values of σ to indicate the start of the second and last stage, $\sigma_{t1} = 0.07$ μm and $\sigma_{t2} = 0.19$ μm. These two thresholds were chosen such that each of them is roughly equivalent to twice the average value of σ in the previous stage. We noticed that occasionally σ can temporarily exceed $\sigma_{t1} =$ 0.07 μm and then still stays below σ_{t1} for a significant amount of time (see Fig. S2). We thus implemented a second criterion for the determination of the onset of stage 2 to account for this scenario: an event of σ exceeding σ_{t1} is not considered as the onset of stage 2 if the value of σ quickly returns to below σ_{t1} and does not exceed σ_{t1} again within the next 8 s (see Fig. S2), which is equivalent to four folds of the longest relaxation time of T4 DNA in 0.5 × TBE.

Calculating ensemble average expansion in each stage. We calculated the evolution of the ensemble average radius of gyration in each stage of type II expansion by first aligning R_g traces of all individual DNA exhibiting type II expansion at the corresponding onset of the stage of interest. Because the distribution of the duration of a given stage is rather broad within a DNA ensemble (see Fig. 4 *E–H* in the article), we calculated $\langle R_g\rangle$ as a function of time starting from the onset of the stage until the number of samples going into the average drops to half of its initial value. The resulting $\langle R_g\rangle$ traces of stage 2 and stage 3 frequently exhibit a small overshoot near the beginning (see Fig. 4*A* in the article). We believe this overshoot is an artifact due to the scheme used to determine the onsets of these two stages because it always occurs exactly at a time (from the beginning of the trace) equivalent to half the width (i.e., 1 s, see Fig. S3) of the sliding window used to calculate σ. This unique feature of the overshoot persists when we changed the width of the sliding window (see Fig. S3).

Statistics and Error Bars. Single molecule experiments are inherently noisy and care must be taken to ensure the trends are statistically significant. Error bars (standard error) given on the data in Fig. 1 of the main text show that the trends are not limited by insufficient ensemble averaging. We replot the data in Fig. 2 of the main text here in Fig. S4 showing less data points but with error bars included to quantify the uncertainty in the measurements.

Histograms of the relaxations times are presented in the main text Fig. 3*G* inset and Fig. 4 *E–H*. Beyond qualitative differences in the overall shape, we can quantitatively compare the distributions by calculating the mean, standard deviation σ and the ratio of σ to the mean. These results are presented in Table S2. The ratio of σ to the mean can be thought of as a normalized measure of the breadth of the distribution. Compared to the unentangled (Type I) case, the entangled chains (Type II) have a wider normalized breadth. Within the entangled chain cases, the distribution becomes significantly less broad as the time in the electric field (T_E) increases from 2 to 30 s. There is then little change in the mean or breadth of the distribution from 30 to 180 s. The trends in σ for the Type II chains is most likely reflective of the evolution of entanglements in the DNA and the sensitivity of the approach to steady state to the initial configuration of the chain, which are consistent with the fact that initial configurations will have varying degrees of spatial segment density variations and these macroion fluctuations drive the instability in the first place.

SI Materials and Methods. ***Channel and DNA preparation.*** Both the 2 μm tall, 200 μm wide, and ∼1 mm long straight channel and the 2 μm tall cross-slot channel were constructed in polydimethylsiloxane (PDMS, Sylgard 184, Dow Corning) using soft lithography on a silicon master (AZ 5214 image reversal photoresist). The geometry of the cross-slot channel is described previously (4). The PDMS channels were soaked in 0.5× Tris-Borate-EDTA (TBE, Omnipure) buffer at 40 °C overnight to eliminate permea-

tion driven flow through the PDMS (5), rinsed and dried briefly, and sealed to a glass coverslide. The microchannels were flushed for 20 min with the experimental buffer via application of potentials at the fluid reservoirs before use. The experimental buffer contains TBE or TE (Tris-EDTA) solution at desired concentration, 0.05% (wt/vol) 10 kDa polyvinylpyrrolidone (PVP, Polysciences) to dynamically coat the channel walls to suppress electroosmotic flow and prevent interactions between channel walls and DNA, and 4% (vol.) beta-mercaptoethanol (BME, Cabiochem) to slow down photobleaching of and photo-induced damage to the stained DNA molecules. T4 DNA molecules (165.6 kbp, Nippon gene) and λ-DNA molecules (48.502 kbp, New England Biolabs) were stained (at a DNA concentration of 0.69 μg/mL) with YOYO-1 (Invitrogen) dye at a basepair to dye ratio of 4:1 and allowed to sit at least overnight. DNA samples were diluted 2 to 10-fold immediately before experiments to reach an optimal concentration for observation.

DNA solution concentration relative to c^*. We can estimate the overlap concentration of our solutions using the formula:

$$c^* = \frac{M_w}{N_A(4/3)\pi R_g^3}, \qquad \text{[S1]}$$

where M_w is molecular weight, N_A is the Avogadro constant, and R_g is the radius of gyration. Taking values of $R_g = 0.69$ μm for λ-DNA and $R_g = 1.3$ μm for T4-DNA results in $c^* = 38$ μg/mL for λ-DNA and $c^* = 19.4$ μg/mL for T4-DNA. As described above, our solutions were typically at concentrations ranging from 0.07–0.35 μg/mL which is significantly below c^* for both molecules.

DNA conformation under electric field. Single DNA molecules under uniform electric fields were observed in the 2 μm tall straight channel using an inverted Zeiss Axiovert 200 microscope with a 63 × NA 1.4 oil-immersed objective (for T4 DNA) or a 100 × NA 1.4 oil-immersed objective (for λ-DNA) and an X-Cite 120 light source. A typical experiment involves first applying a weak DC electric field of 15 V/cm for 5 min to electrophoretically flush out any DNA molecules that have previously experienced high electric field and to introduce equilibrium DNA molecules into the microchannel, then switching to the desired field strength (DC or AC), waiting for 3 min, and starting image acquisition. In experiments with AC electric fields, a DC offset of about 5 V/cm was superimposed onto the AC square-wave in order to create a net electrophoretic motion of DNA molecules such that they can be continuously brought into the field of view. DNA images were collected using a Hamamatsu EB-CCD camera (model 7190-21) and NIH image software. The CCD camera has a fixed exposure time (1/30 s) and thus cannot be used to observe the conformation of DNA molecules under fast electrophoretic motion (especially at $E > 50$ V/cm, see Fig. S5). As a result, once a DNA molecule of interest enters the field of view, we switched off the electric field to stop the motion of the molecule, captured the DNA conformation in the first frame where the DNA image is not blurred (i.e., within 1/30 s of stopping the electric field, see Fig. S5), and turned on the field again. The electric field was kept off for less than 0.5 s during this process, ensuring that no significant expansion of the DNA has occurred before the field is switched back on.

Expansion of compressed T4 DNA. A weak DC electric field of 15 V/cm was applied for 5 min to electrophoretically drive T4 DNA molecules at equilibrium into the 2 μm tall straight channel. A 10 Hz AC square-wave electric field with no DC offset was then applied for a desired duration to compress the T4 DNA molecules. After the field is switched off, the expansion of the compressed T4 DNA was observed. We examined the expansion dynamics as functions of both the root-mean-square field strength E_{rms} and the duration T_E of the AC electric field. We chose to use the 10 Hz AC electric field to compress T4 DNA for two major reasons: (*i*) DNA molecules of interest stay in the field of view while being compressed under this field condition, allowing us to precisely control the duration of the applied electric field, and (*ii*) the compression is not significantly suppressed at a frequency of 10 Hz.

Stretching of compressed T4 DNA. To stretch the compacted DNA we use a planar homogeneous elongational field generated in a 2 μm tall cross-slot channel (4) to stretch T4 DNA under a strain rate $\dot{\epsilon}$ of 1.1 s^{-1}. This strain rate corresponds to a Deborah number, $De = \tau\dot{\epsilon}$, of 2.0 where τ is the longest relaxation time of unentangled T4 DNA (1.9 s). Fig. S6 *A* and *B* show typical traces of the extension of individual molecules vs. strain for uncompressed T4 DNA and T4 DNA initially compressed under a 10 Hz AC electric field of $E_{\text{rms}} = 200$ V/cm for 30 s, respectively. We see that the compressed DNA molecules extend dramatically slower comparing to the uncompressed DNA under the same strain rate. While most uncompressed T4 DNA reach steady-state extension within 10 units of strain, many of the compressed globules (e.g., the red curve in Fig. S6*B*) do not show any stretching even after an applied strain of 25. The entangled DNA usually follows a unique stretching pathway in which the two chain ends constantly protrude out and the compact core of the globule shrinks (Fig. S6*C*, also Movie S3). These dynamics are qualitatively similar to the "protrusion nucleation" dynamics recently observed in simulations of the globule-stretch transition of polymers in a poor solvent subject to elongational flow (6). The compact cores in nearly all of these molecules do not vanish when steady states are reached but evolve into a single or multiple (occurs rarely) intramolecular knots represented by local bright spots (Fig. S6*C*, indicated by yellow arrows) along the extended DNA chain. Both the strong resistance of the globule to external forces and the knots observed on the stretched chains provide solid evidence that entanglements are present.

To obtain the stretching data, we used a 2 μm tall PDMS cross-slot channel to stretch compressed T4 DNA molecules in 0.5 × TBE. The mechanism of using electric field to stretch single DNA molecules in this device has been described in details in a previous work (4). When symmetric potentials are applied to the channel in a manner as shown in Fig. S7, a local planar homogeneous elongational electric field with a stagnation point can be obtained within the intersection and uniform fields in the four straight arms. T4 DNA molecules at equilibrium were first electrophoretically driven into the top straight channel with small DC potentials (yield about 20 V/cm in the straight arm). We then applied 10 Hz AC square-wave electric potentials that generate an AC electric field of $E_{\text{rms}} = 200$ V/cm to compress these molecules inside the top channel for 30 s (Fig. S7*A*). Once the AC potentials were switched off, we immediately applied symmetric DC potentials (Fig. S7*B*) to drive a compressed T4 DNA molecule into the intersection and stretch it using the homogeneous elongational electric field (4) with a strain rate of 1.1 s^{-1} (corresponding to a Deborah number of 2.0). The DC field applied during stretching is well below the strengths at which DNA collapse is induced. In fact, the field is zero at the center of the cross-slot (a field stagnation point, also the center of a stretched DNA molecule) and increases to 14 V/cm at each end of a stretched T4 DNA molecule that has a steady-state extension of about 50 μm under a Deborah number of 2.0.

1. Stellwagen N, Gelfi C, Righetti P (1997) The free solution mobility of DNA. *Biopolymers* 42:687–703.
2. Tang J, Levy S, Trahan D, Jones J, Craighead H, Doyle P (2010) Revisiting the conformation and dynamics of DNA in slit-like confinement. *Macromolecules* 43:7368–7377.
3. Mitnik L, Heller C, Prost J, Viovy J-L (1995) Segregation in DNA solutions induced by electric-fields. *Science* 267:219–222.
4. Tang J, Trahan D, Doyle P (2010) Coil-stretch transition of DNA molecules in slit-like confinement. *Macromolecules* 43:3081–3089.
5. Randall G, Doyle P (2005) Permeation-driven flow in poly(dimethylsiloxane) microfluidic devices. *Proc Natl Acad Sci USA* 102:10813–10818.
6. Sing CE, Alexander-Katz A (2010) Globule-stretch transitions of collapsed polymers in elongational flow fields. *Macromolecules* 43:3532–3541.

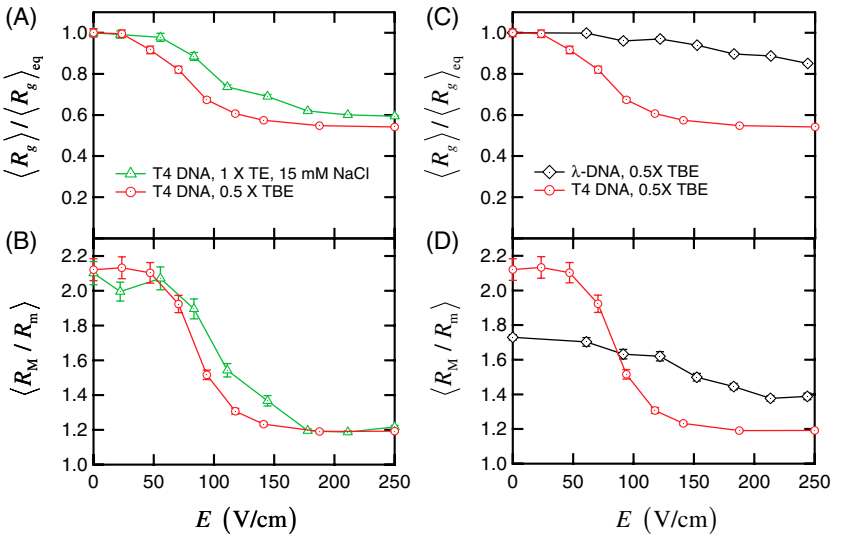

Fig. S1. (*A*) and (*B*) Conformation of T4 DNA under uniform DC electric fields in 0.5 × TBE and in 1 × TE, 15 mM NaCl: (*A*) ensemble average radius of gyration R_g of T4 DNA (normalized by the equilibrium average) and (*B*) the corresponding average ratio between the major and minor axes $\langle R_M/R_m \rangle$ as functions of the field strength E. The two buffers have similar ionic strength. (*C*) and (*D*) Conformation of T4 DNA and λ-DNA under uniform DC electric fields in 0.5 × TBE: (*C*) ensemble average radius of gyration R_g (normalized by the equilibrium average) and (*D*) the corresponding average ratio between the major and minor axes $\langle R_M/R_m \rangle$ as functions of the field strength E.

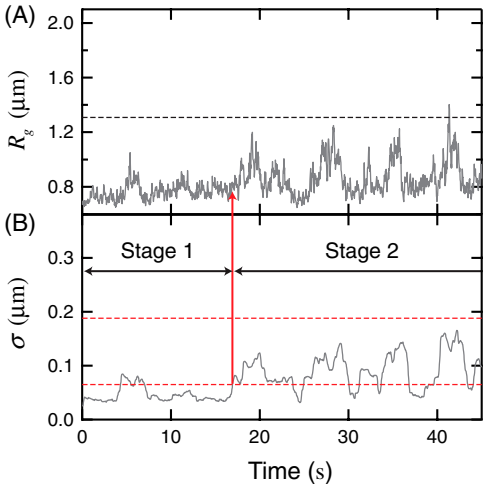

Fig. S2. (*A*) R_g trace of a T4 DNA molecule that exhibits type II expansion. The molecule is compressed using a 10 Hz AC electric field of $E_{rms} = 200$ V/cm for $T_E = 30$ s. The dashed line indicates the equilibrium average radius of gyration. (*B*) The corresponding local standard deviation σ calculated using a sliding window of 2 s and the first two expansion stages (the molecule does not enter stage 3 during the 45 s of observation). The two red dashed lines indicate the two thresholds ($\sigma_{t1} = 0.07$ μm and $\sigma_{t2} = 0.19$ μm) used to determine the onset of stage 2 and stage 3. The value of σ first exceeds σ_{t1} at about 5 s but then quickly returns to its initial magnitude and does not exceed σ_{t1} again in the next 8 s. As a result, the time point at which σ first exceeds σ_{t1} is not considered as the onset of stage 2.

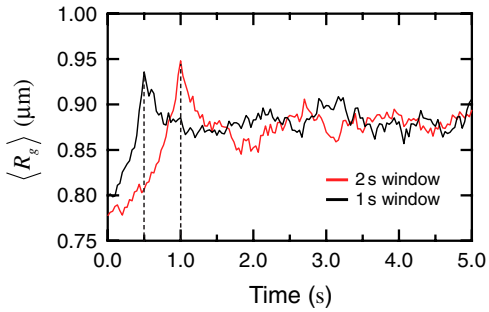

Fig. S3. Ensemble average radius of gyration vs. time in the second stage of type II expansion for the DNA ensemble compressed under $E_{rms} = 200$ V/cm for 10 s. Results calculated from two sliding windows with different width (1 s and 2 s) are shown. Both $\langle R_g \rangle$ traces show an overshoot at a time point that equals to half of the corresponding width of the sliding window.

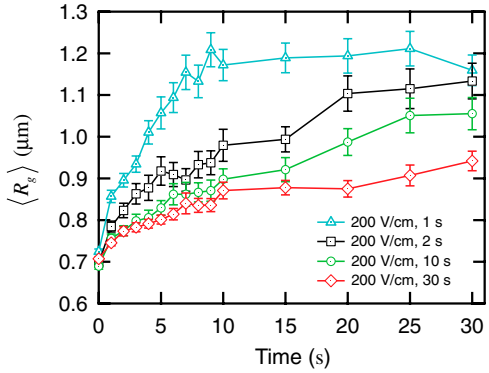

Fig. S4. Sample data with error bars (standard error) of $\langle R_g \rangle$ of T4 DNA compressed using a 10 Hz square-wave electric field of $E_{rms} = 200$ V/cm for four different durations: $T_E = 1$ s, 2 s, 10 s, and 30 s.

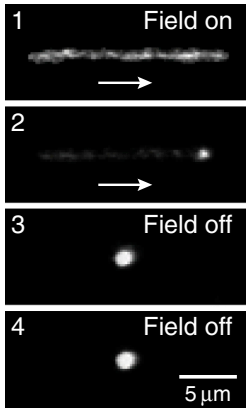

Fig. S5. Snap shots of a T4 DNA molecule in four consecutive frames during the course of stopping the applied DC electric field (200 V/cm) and capturing the conformation of the compressed DNA. Each frame is an average of signal for 1/30 s. Frame 1: the electric field is on and the DNA image is blurred due to the fast electrophoretic motion of the molecule and the fixed exposure time (1/30 s) of the CCD camera. Frame 2: the field is switched off during the second 1/30 s and the bright spot in the image suggests that the DNA has stopped moving at the end of the 1/30 s. The arrows in frame 1 and 2 indicate the direction of DNA electrophoresis. Frame 3 and 4: the compressed DNA remains still and its conformation can be clearly seen. The first frame (i.e., frame 3) in which the DNA is not blurred is captured for our measurement of the DNA conformation.

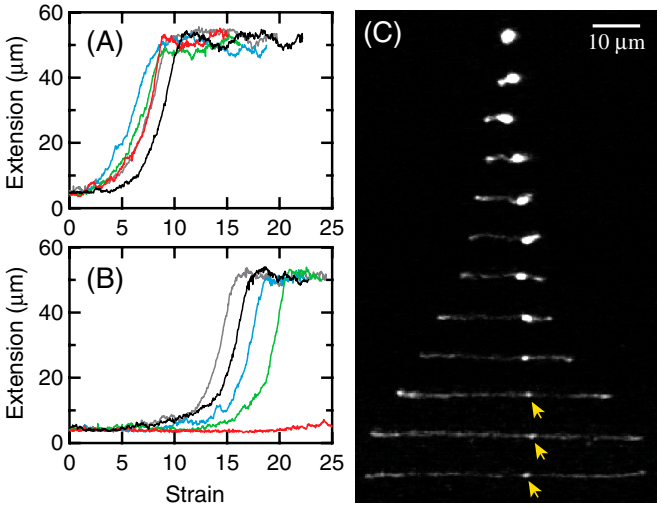

Fig. S6. Stretching of T4 DNA molecules using a homogeneous elongational field in a 2 μm tall cross-slot channel. (*A*) Traces of extension vs. strain for five noncompressed T4 DNA molecules. (*B*) Traces of extension vs. strain for five T4 DNA molecules that are compressed with an AC electric field of 10 Hz, E_{rms} = 200 V/cm for 30 s. All molecules are stretched using a strain rate of 1.1 s^{-1} or a Deborah number of De = 2.0. (*C*) Snap shots of the stretching process of the initially compressed DNA corresponding to the black curve in (*B*). The corresponding strain for each image is 0, 6.0, 8.8, 11.6, 13.0, 13.7, 14.4, 15.1, 15.7, 16.4, 17.2, and 19.4 from top to bottom. The yellow arrows indicate the knot in the molecule.

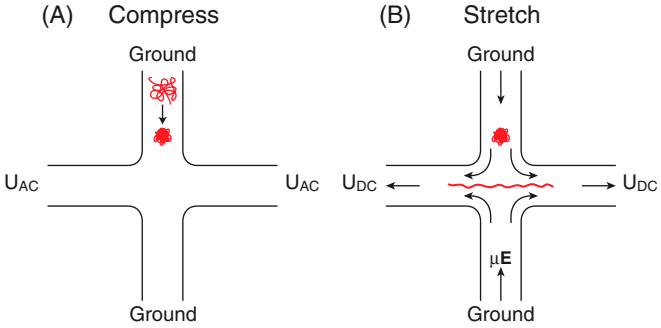

Fig. S7. Schematics of the T4 DNA stretching experiments. (*A*) An AC square-wave potential is applied to the cross-slot channel to generate a uniform AC electric field of E_{rms} = 200 V/cm in the top straight arm of the channel. T4 DNA molecules that are present inside the top arm are compressed to globules. The AC field is applied for 30 s. (*B*) After the AC potential is switched off, a DC potential is immediately applied to drive a compressed molecule into the intersection and stretch it with the planar homogeneous elongational electric field near the stagnation point. Arrows in (*B*) indicate the direction of the DNA electrophoretic velocity (μE).

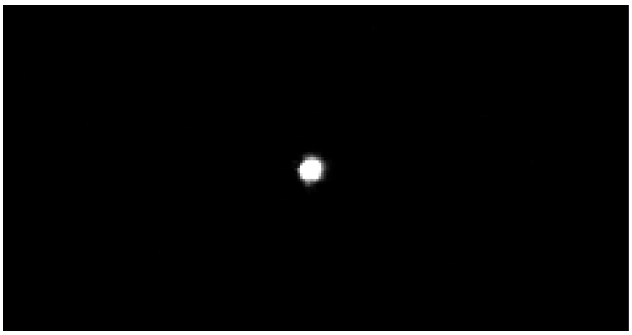

Movie S1. Compression of a T4 DNA molecule in 0.5 × TBE by applying a 10 Hz AC electric field of E_{rms} = 200 V/cm for 1 s.

Movie S1 (AVI)

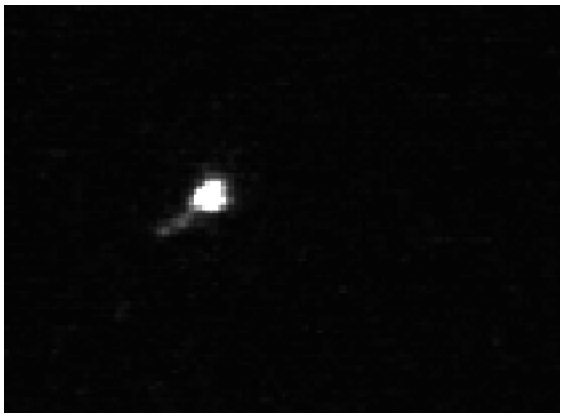

Movie S2. Type II expansion of the T4 DNA molecule corresponding to the R_g trace shown in Fig. 3*C* in the article.

Movie S2 (AVI)

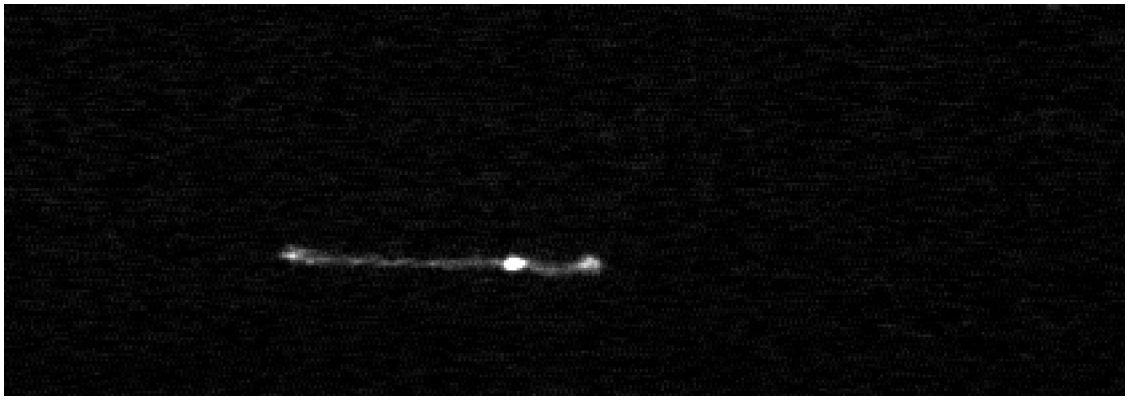

Movie S3. Electrophoretic stretching of a T4 DNA molecule that is initially compressed with an AC electric field of $E_{rms} = 200$ V/cm for 30 s in 0.5 × TBE and in the cross-slot channel at a strain rate of 1.1 s^{-1}.

Movie S3 (AVI)

Table S1. The initial average radius of gyration and the proportion of DNA molecules exhibiting type II expansion for T4 DNA ensembles compressed under AC electric field with various values of E_{rms} and T_E

E_{rms} (V/cm)	T_E (s)	$\langle R_{g,0} \rangle$ (μm)	Percentage of type II expansion
150	1	0.86 ± 0.03	9%
150	10	0.77 ± 0.01	77%
200	1	0.73 ± 0.01	56%
200	2	0.70 ± 0.01	82%
200	10	0.69 ± 0.01	91%
200	30	0.71 ± 0.01	95%
200	180	0.69 ± 0.01	99%

Table S2. The ensemble average and standard deviation (σ) of the characterization time scales for type I (the time constant τ obtained by fitting the time trace of $(\langle R_g^2\rangle_{eq} - R_g^2)/\langle R_g^2\rangle_{eq}$) and type II expansion (the duration τ_1 of the first stage)

E_{rms} (V/cm)	T_E (s)	Expansion type	Mean (s)	σ (s)	σ/mean
150	1	I	$\langle\tau\rangle = 2.4$	1.3	0.56
200	2	II	$\langle\tau_1\rangle = 6.4$	8.7	1.36
200	10	II	$\langle\tau_1\rangle = 11.5$	11.3	0.98
200	30	II	$\langle\tau_1\rangle = 19.7$	14.6	0.74
200	180	II	$\langle\tau_1\rangle = 18.4$	15.2	0.83